# Laser-Generated Ultrashort Multimegagauss Magnetic Pulses in Plasmas

A. S. Sandhu,[1] A. K. Dharmadhikari,[1] P. P. Rajeev,[1] G. R. Kumar,[1] S. Sengupta,[2] A. Das,[2] and P. K. Kaw[2]

[1]*Tata Institute of Fundamental Research, 1 Homi Bhabha Road, Mumbai 400 005, India*

[2]*Institute for Plasma Research, Bhat, Gandhinagar, Ahmedabad 382428, India*

(Received 13 April 2002; published 11 November 2002)

We demonstrate ultrashort (6 ps), multimegagauss (27 MG) magnetic pulses generated upon interaction of an intense laser pulse ($10^{16}$ W cm$^{-2}$, 100 fs) with a solid target. The temporal evolution of these giant fields generated near the critical layer is obtained with the highest resolution reported thus far. Particle-in-cell simulations and phenomenological modeling is used to explain the results. The first direct observations of anomalously rapid damping of plasma shielding currents produced in response to the hot electron currents penetrating the bulk plasma are presented.

DOI: 10.1103/PhysRevLett.89.225002 PACS numbers: 52.38.Fz, 52.65.Rr, 52.70.Ds, 52.70.Kz

The largest magnetic fields available terrestrially ($\sim 10^8$ G) are generated by explosive ionization of a solid target with an intense ultrashort laser pulse [1]. Since the first observation of such magnetic fields, their origin, magnitudes, and other qualitative features have attracted considerable attention [2]. Recently, subpicosecond laser produced solid plasmas have provided a new experimental facet to these studies. Magnetic fields up to gigagauss magnitudes have been predicted in the overdense region of a solid target [3]. Little, however, is known about the temporal evolution of these huge magnetic fields generated around the critical layer. These fields play a crucial role in electron transport [4] and are, therefore, important for potential applications in hybrid confinement and fast ignition [5] schemes of laser fusion.

In this Letter, we present first experimental measurements of the temporal evolution of megagauss magnetic fields generated *at the critical layer*, on femtosecond time scales. The field generation and decay mechanisms are identified and the role of resonance absorption is examined. The initial buildup of magnetic field due to direct laser radiation effects is calculated using LPIC++ code [6], and the results are found to be in good agreement with the experiment. The field evolution is explained to be due to currents generated by fast electrons [7] and plasma return currents damped by turbulence induced resistivity [8]. The first direct observation of anomalously rapid damping of return currents, which may have important consequences for laser fusion, is reported. We demonstrate ultrashort, megagauss magnetic pulses, with 6 ps (FWHM) duration and a peak magnitude of 27 MG generated by a *p*-polarized laser pulse.

A linearly polarized pump pulse (806 nm, 100 fs) incident at 55° is focused on a solid aluminum target with typical intensities of $10^{16}$ W cm$^{-2}$ (Fig. 1). A small part of the laser is used to generate a linearly polarized, second harmonic (403 nm) probe pulse. The probe pulse incident at 50° is focused to an intensity of $5 \times 10^{12}$ W cm$^{-2}$ and is spatially overlapped with the pump spot. In this configuration, the probe penetrates beyond the critical density ($n_c$) for pump (i.e., up to $1.65 n_c^{(806)}$ or $0.4 n_c^{(403)}$; see inset Fig. 1). The long term contrast for the pump is $10^5$. The second harmonic probe is expected to have a contrast of $10^{10}$.

The novel features of this experiment are as follows: (i) We are able to examine the generated magnetic field on either side of the critical layer by using the second harmonic of the laser as a nontangential probe; (ii) we identify zero-delay time precisely and obtain high-resolution data for temporal evolution; and (iii) we examine, using oblique pump incidence, the role of resonance absorption (RA). To our knowledge, only one laboratory has hitherto reported [9] pump-probe magnetic fields measurements on picosecond time scales (using 1 ps duration laser pulse). However, these measurements

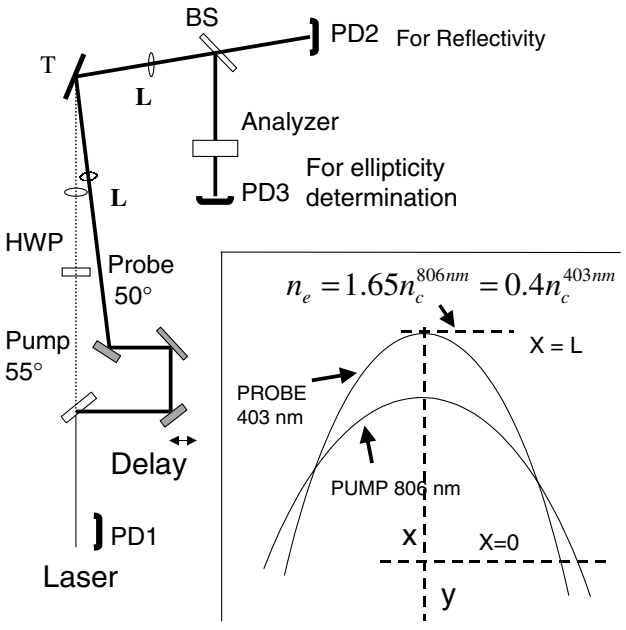


FIG. 1. Experimental setup: target (T), lens (L), beam splitter (BS), photodiode (PD), half-wave plate (HWP). Inset represents pump and probe paths in plasma.

  

were confined to an underdense plasma region ($n_e = 4 \times 10^{19}$ cm$^{-3}$) and the diagnostics employed limited the temporal resolution to ~3 ps. We emphasize our probing technique, because magnetic field generation primarily occurs near the critical surface ($n_e \sim 10^{21}$ cm$^{-3}$), the region of maximum laser absorption [7,10]. Moreover, it is the magnetic field in the overdense region that determines hot electron transport into the bulk, which is crucial for fusion related issues.

We measure the change in the polarization state of a probe pulse induced by the "dc" magnetic field in the plasma. We observe no significant Faraday rotation (within detection sensitivity of 0.25°) but large and easily measurable ellipticity change. This indicates that $B$ is essentially perpendicular to $k$, in agreement with previous reports for RA generated magnetic fields [11]. Therefore the standard Cotton-Mouton polarimetry formulation [12] is used to deduce the magnetic field. The spot radii for pump and probe are 15 and 10 $\mu$m, respectively. The amplitude and polarization of the reflected probe is simultaneously monitored by splitting it into two arms, one measuring the reflectivity with a photodiode (PD2), and the other measuring the polarization state using an analyzer (extinction ratio $10^{-5}$) in front of another identical photodiode (PD3), as shown in Fig. 1. The photodiode PD1 measures the shot to shot laser fluctuations. The ratio $R = (\text{signal PD3})/(\text{signal PD2})$ is used in data acquisition and analysis so as to account for plasma reflectivity variation as a function of time delay. Initially, the ellipticity ($\beta$) is determined at various fixed delay positions (in steps of 0.5 ps) by studying ratio $R$ as a function of analyzer angle, which varies as $\cos^2\theta + \beta^2 \sin^2\theta$. Higher temporal resolution ellipticity data is obtained using fixed analyzer positions ($\theta = 0°$, 45°, 90°) and acquiring $R$ as a function of time delay. The plasma propagation and refraction effect of the probe yields a small baseline contribution to ellipticity which is observed to be a maximum of 0.1 at negative delay. This contribution is subtracted from the ellipticity data to get purely pump generated magnetic field induced ellipticity which is shown in the inset of Fig. 2. We also calculate the contribution to induced ellipticity from plasma propagation and refraction effects [13] and the resulting value [14] is close to the baseline which was subtracted above.

Figure 2 presents the temporal evolution of the magnetic field. The inset shows reflectivity and induced ellipticity of the probe for a $p$-polarized pump. The sharp reflectivity dip is used to independently establish the start of the magnetic pulse. The magnetic field is derived from induced ellipticity ($\beta$) for our experimental conditions using [12] $\beta(t) = (e^2/m_e c^3 \omega n_c) \int n_e(l,t) B^2(l,t) dl$. The magnetic field is deduced assuming a spatially uniform $B$ over a linear density gradient $n_e(x) = 0.4 n_c^{(403)}(x/L)$, where $L$ is the plasma slab length, as shown in the inset of Fig. 1. The factor $0.4 n_c^{(403)}$ corresponds to the turning point density for the 403 nm probe. The assumption of uniformity over linear density profile serves to yield a conservative estimate of the magnetic field. We integrate over the trajectory in the plasma, $dl = \sqrt{1 + y'^2}\,dx$, where $y' = \sin\theta_0 / \sqrt{\epsilon(x) - \sin^2\theta_0}$ , $\epsilon(x)$ being the dielectric function. The plasma expansion velocity is estimated to be $5 \times 10^7$ cm/s from Doppler shift measurements of the reflected probe. The magnetic field as a function of time delay is obtained as $B(t) = [m_e^2 c^3 \omega \beta(t)/0.69 e^2 L(t)]^{1/2}$, where $L(t) = L_0 + v_{\text{exp}} t$ and $L_0$ is 1 $\mu$m. From the results shown in Fig. 2, the magnetic field pulse generated by the $p$-polarized pump has a peak value of 27 MG and duration (FWHM) of 6 ps. In comparison, the $s$-polarized pump results in a peak value of 14 MG. We now present a possible interpretation of these results.

Recent multidimensional particle-in-cell (PIC) simulations [7] have shown that, in ultrashort laser-plasma experiments, hot electrons are generated at the laser-plasma interface by RA and/or vacuum heating mechanisms and propagate into the cold overdense plasma exciting neutralizing return currents. The mechanism of quasistatic magnetic field generation can be understood by the following equation:

$$\frac{\partial \vec{B}}{\partial t} = -\nabla \times \left( \frac{\vec{j} \times \vec{B}}{n_e e} \right) + \frac{c}{n_e e} (\vec{\nabla} T_e \times \vec{\nabla} n_e) + \frac{c}{\sigma} (\vec{\nabla} \times \vec{j}_{\text{hot}}) + \frac{c^2}{4\pi\sigma} \nabla^2 \vec{B}, \quad (1)$$

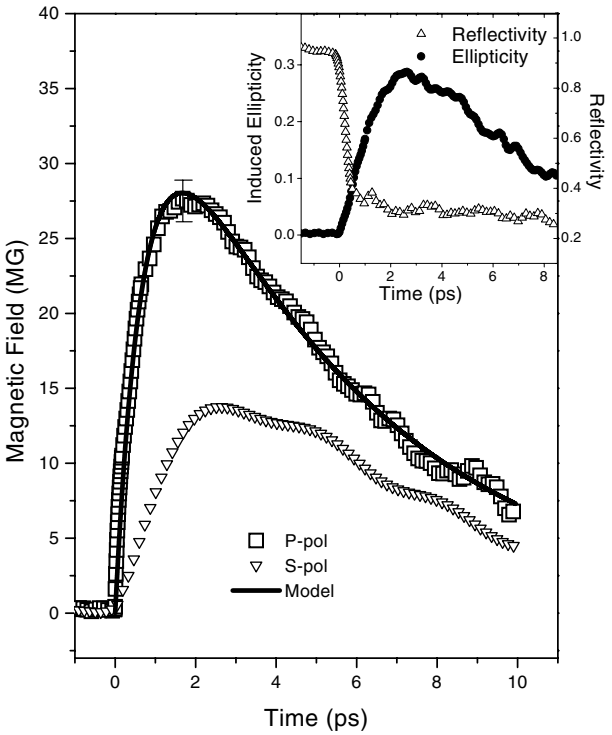


FIG. 2. Magnetic field pulse profile for $p$- and $s$-polarized pump laser with intensity of $1.1 \times 10^{16}$ W cm$^{-2}$. Solid line shows the fit for the $p$-polarized case using a phenomenological model. The inset shows the reflectivity and induced ellipticity of the probe as a function of delay time.

Equation (1) is derived by taking the curl of the equation of motion of background plasma electrons that carry the plasma shielding currents, $\vec{j}_p = (c/4\pi)\vec{\nabla} \times \vec{B} - \vec{j}_{\rm hot}$. The Hall effect drive (first term) arises [15] due to the high frequency electromagnetic fields in the plasma excited by the laser pulse [16] and due to any electron magnetohydrodynamic (EMHD) turbulence effects generated by the interaction of hot electron currents with the return shielding currents [7]. The second term is the thermoelectric source and the third term is the source due to hot electrons; the last term gives the magnetic field decay due to resistive damping of the plasma shielding currents ($\sigma^{-1}$ being the background plasma resistivity). We estimate the part of Hall effect drive due to high frequency electromagnetic fields by taking a cycle-averaged product $\vec{\nabla} \times \langle(\vec{j}_h \times \vec{B}_h)/n_e e\rangle$, inside the plasma. This part has been shown by others [16,17] to be proportional to the dissipation rate and intensity of the excited plasma waves. The magnitudes of $j_h$, $B_h$ are obtained by carrying out a simplified one-dimensional PIC simulation using the laser-plasma interaction code LPIC++. In the simulation, a $p$-polarized light pulse with $\sin^2$ envelope and 100 fs FWHM laser pulse is incident at an angle of 55° on a linear density ramp. Figure 3(a) shows numerically obtained spatial and temporal profiles of the quasisteady state magnetic field. The magnitudes of $|B|$ and $|\partial B/\partial t|$ obtained from simulation (viz. 1.2 MG and 22 MG/ps at 150 fs, respectively) agree well with our experimental values for $p$-polarized light [Fig. 3(b)]. Beyond 150 fs, the simulation shows saturation of the $B$ field, whereas the experiment does not; this is because the simulations are simplified and one dimensional and do not retain the physics associated with the other source terms in Eq. (1).

We now discuss these other source terms. The second term in Eq. (1) is estimated assuming a temperature gradient of 100 eV over a transverse scale of 15 $\mu$m (pump spot radius) and density gradient of $10^{21}$ cm$^{-3}$ over 1 $\mu$m in the normal direction. This gives $|\partial B/\partial t| \sim$ 0.05 MG/ps, which is much smaller than the experimental results. Hence, the thermoelectric source term is neglected in subsequent analysis. The remaining terms in Eq. (1) (viz. the hot electron source, the magnetic diffusion, and the $\vec{j} \times \vec{B}$ terms due to dynamo action of residual quasistatic EMHD turbulence) remain finite even after the pump pulse is removed and may be modeled by a phenomenological zero-dimensional equation $\partial B/\partial t = S(t) - B/\tau$, where $B/\tau$ is a 0D representation of the magnetic diffusion term and $S(t)$ is the source term. Taking $S(t) = S_0 \exp(-t/t_0)$, we get $B(t) = S_0(1/\tau - 1/t_0)^{-1}[\exp(-t/t_0) - \exp(-t/\tau)]$. The first exponential term in the above the equation denotes the natural decay of the source terms, and the second describes the resistive decay of the fields generated by the plasma return currents. As shown in Fig. 2, this expression gives an excellent fit to our experimental data for the $p$-polarized

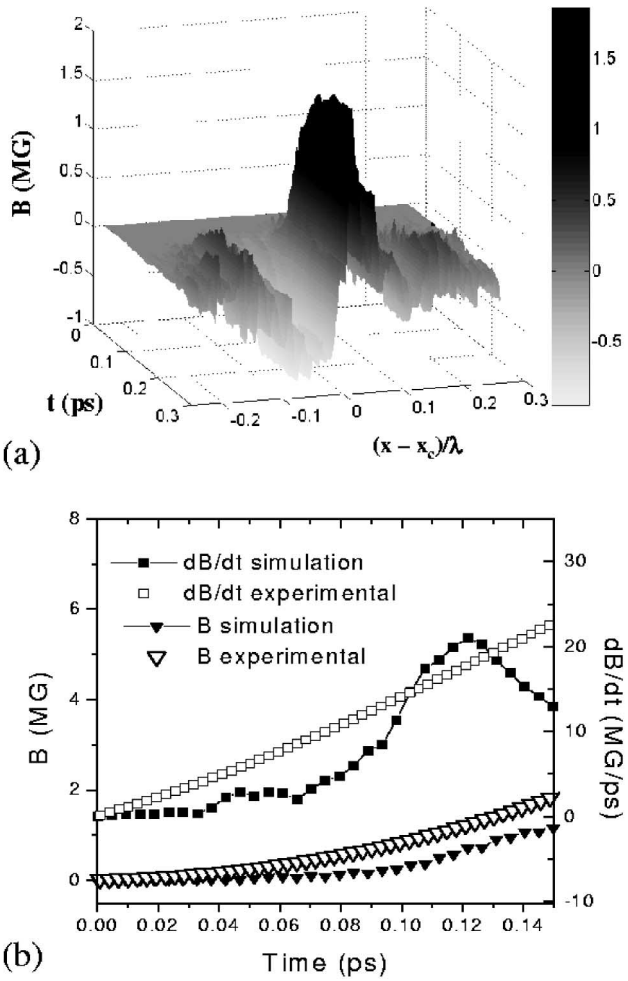


FIG. 3. (a) The temporal and spatial profile of magnetic field obtained using the LPIC++ code ($x = x_c$ is the critical layer). (b) Comparison of $B$ and $dB/dt$ obtained using LPIC++ simulation with experimental results.

pump with $S_0 = 53.7$ MG/ps, $t_0 = 0.7$ ps, and $\tau = 5.6$ ps. To get an insight into these numerical values, we estimate conductivity $\sigma$ from the magnetic diffusion term. Assuming that the currents propagate axially (normal to vacuum-plasma interface) in channels of radius $\Delta r \sim$ focal spot size, we have $\tau \sim (4\pi\sigma/c^2)(\Delta r)^2$, which for $\Delta r \approx 15$ $\mu$m and our best fit value $\tau \sim 5.6$ ps gives $\sigma \sim 1.8 \times 10^{14}$ s$^{-1}$. This value of $\sigma$ may be compared with $\sigma_{\rm solid}$ or $\sigma_{\rm classical}$ observed [18] at $T_e = 100$ eV which has a value $\approx 4.2 \times 10^{15}$ s$^{-1}$. Thus, the observed $\sigma$ is an order of magnitude smaller than expected. This enhanced resistivity may result either because the current loops influencing our $B$ field measurements are extending deeper into denser and colder plasma where the classical plasma resistivity is higher or because locally, in plasma regions considered by us, the resistivity is anomalously large due to EMHD turbulence effects [7,8]. However, a survey of measurements of classical resistivity in dense cold Al plasmas [18] reveals that resistivity shows a

saturation behavior with a maximum value of 260 $\mu\Omega$ cm for $T_e \approx 40$ eV (implying $\sigma_{\text{classical}} \geq 3.5 \times 10^{15}$ s$^{-1}$); hence, the first interpretation is untenable for our observations. On the other hand, an upper estimate of anomalous resistivity due to turbulence of electron waves may be obtained by taking the effective collision frequency due to collective effects $\nu_{\text{eff}} \sim f\omega_p$ (where $f$ is a fraction of order unity) and is in reasonable agreement with our measured value of $\sigma$. Hence, one is forced to conclude that a turbulence induced anomalous resistivity has been observed in these experiments. To get an independent estimate of $S_0$, which is the maximum value of the source term $|(c/\sigma)(\vec{\nabla} \times \vec{j}_{\text{hot}})|$, we now evaluate $j_{\text{hot}}$. Assuming a conversion fraction $f_a$ of incident energy into hot electrons, we have $j_{\text{hot}} \approx f_a eI/T_{\text{hot}}$. Taking $f_a \sim 0.3$ and $T_{\text{hot}} \sim 20$ keV, we have $|j_{\text{hot}}| \sim 4.5 \times 10^{20}$ statampere/cm$^2$. Taking $|\vec{\nabla}| \sim 1/15\ \mu\text{m}^{-1}$ and the value of $\sigma$ obtained above, we get the estimate of $S_0$ as $\sim$50 MG/ps; this estimate closely matches the value obtained by fitting the 0D model to experiments.

The experimental results for $s$ polarization (smaller values of $|\partial B/\partial t|$ in Fig. 2) need an independent discussion. $s$-polarized light can also lead to plasma wave excitation and associated quasisteady state $B$-field generating currents, provided there is a rippling of the critical surface [19]. The intensity of the excited plasma wave is proportional to the fractional absorption of the light wave which, as shown in Ref. [20], is lower for $s$-polarized light. This results in lower $|\partial B/\partial t|$ and, hence, a lower $|\vec{B}|$.

In conclusion, we have measured and characterized picosecond megagauss magnetic pulses generated by the interaction of ultrashort laser pulse with a solid. Our measurements extend to the overdense region of the target and, hence, are of relevance to electron transport and fusion related issues. The experimentally observed rise times and magnitude of magnetic fields closely follow theoretical estimates and simulations. We also observe, for the first time, anomalously rapid damping of return plasma shielding currents produced in response to the hot electron currents penetrating the bulk plasma. This is a topic of considerable significance to the fast ignition scheme of laser fusion and may actually be the first experimental indication that turbulence induced anomalous resistivity mechanisms are operating. More detailed measurements and simulations are required to pin down these mechanisms further. Such ultrashort, localized magnetic fields are also useful for investigating magnetic precession and reversal dynamics [22], and testing astrophysical theories in the laboratory [23]. The intensities used in our experiments are easily realizable with modern kilohertz repetition rate femtosecond lasers, and we foresee exciting applications for these magnetic pulses.

We thank J. Meyer-ter-Vehn and T. Schlegel for the LPIC++ code, and D. Mathur and S. Maiti for useful suggestions. Our laser was partially funded by the Department of Science and Technology.

[1] M. Tatarakis *et al.*, Nature (London) **415**, 280 (2002).
[2] J. A. Stamper, Laser Part. Beams **9**, 841 (1991).
[3] S. C. Wilks *et al.*, Phys. Rev. Lett. **69**, 1383 (1992).
[4] R. J. Mason and M. Tabak, Phys. Rev. Lett. **80**, 524 (1998); J. R. Davies *et al.*, Phys. Rev. E **59**, 6032 (1999).
[5] M. Tabak *et al.*, Phys. Plasmas **1**, 1626 (1994).
[6] R. Lichters *et al.*, Phys. Plasmas **3**, 3425 (1996).
[7] Y. Sentoku *et al.*, Phys. Plasmas **6**, 2855 (1999); Y. Sentoku *et al.*, Phys. Rev. E **65**, 046408 (2002).
[8] J. F. Drake *et al.*, Phys. Rev. Lett. **73**, 1251 (1994); A. Das and P. H. Diamond, Phys. Plasmas **7**, 170 (2000).
[9] M. Borghesi *et al.*, Phys. Rev. Lett. **81**, 112 (1998); Z. Najmudin *et al.*, Phys. Rev. Lett. **87**, 215004 (2001).
[10] W. L. Kruer, *The Physics of Laser-Plasma Interactions* (Addison-Wesley, New York, 1988).
[11] Y. Sakagami *et al.*, Phys. Rev. A **21**, 822 (1980); M. Tatarakis *et al.*, Phys. Plasmas **9**, 2244 (2002 ).
[12] I. H. Hutchinson, *Principles of Plasma Diagnostics* (Cambridge University Press, New York, 1987); S. E. Segre, Phys. Plasmas **3**, 1182 (1996).
[13] R. H. Lehmberg and J. A. Stamper, Phys. Fluids **21**, 814 (1978).
[14] The effective phase difference from Helmholtz solver yields for our parameters, $\phi_{\max} = 0.12$ rad, implying $\beta = 0.07$.
[15] A. S. Kingsep *et al.*, *Reviews of Plasma Physics* (Consultant Bureau, New York, 1990).
[16] W. Woo and J. S. DeGroot, Phys. Fluids **21**, 124 (1978).
[17] J. J. Thompson *et al.*, Phys. Rev. Lett. **35**, 663 (1975).
[18] H. M. Milchberg *et al.*, Phys. Rev. Lett. **61**, 2364 (1988); A. Ng *et al.*, Phys. Rev. Lett. **57**, 1595 (1986).
[19] E. J. Valeo and K. G. Estabrook, Phys. Rev. Lett. **34**, 1008 (1975).
[20] The ratio of fractional absorption of $s$-polarized [21] to that of $p$-polarized light [10] for incidence angle of 55° is $f_s/f_p \approx \alpha(\delta n/n_0)^2$, where $\alpha \approx 2.3F(k)$. $F(k)$ is a factor of order unity. To explain the experimentally observed $|\partial\vec{B}/\partial t|_{s,\max} \approx 0.1 \times |\partial\vec{B}/\partial t|_{p,\max} \approx 2$ MG/ps for $s$-polarized light (which implies $f_s/f_p \approx 0.1$), we need $\delta n/n_0 \sim 13\%$, a reasonably sized ripple on the critical surface.
[21] R. A. Cairns, Plasma Phys. **20**, 991 (1978).
[22] C. H. Back *et al.*, Science **285**, 864 (1999).
[23] D. Lai, Rev. Mod. Phys. **73**, 629 (2001).